

Robust, Superamphiphobic Fabric with Multiple Self-Healing Ability against Both Physical and Chemical Damages

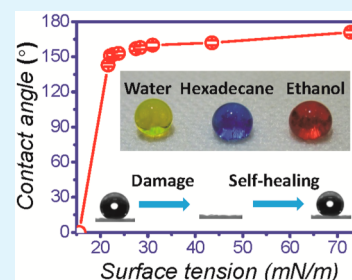
Hongxia Wang, Hua Zhou, Adrian Gestos, Jian Fang, and Tong Lin*

Institute for Frontier Materials, Deakin University, Geelong VIC 3216, Australia

S Supporting Information

ABSTRACT: Superamphiphobic coatings with excellent repellency to low surface tension liquids and multiple self-healing abilities are very useful for practical applications, but remain challenging to realize. Previous papers on self-healing superamphiphobic coatings have demonstrated limited liquid repellency with single self-healing ability against either physical or chemical damage. Herein, we describe a superamphiphobic fabric that has remarkable multi-self-healing ability against both physical and chemical damages. The superamphiphobicity was prepared by a two-step surface coating technique. Fabric after coating treatment showed exceptional liquid-repellency to low surface tension liquids including ethanol. The fabric coating was also durable to withstand 200 cycles of laundries and 5000 cycles of Martindale abrasion without apparently changing the superamphiphobicity. This highly robust, superamphiphobic fabric may find applications for the development of “smart” functional textiles for various applications.

KEYWORDS: superamphiphobic, self-healing, fabric, coating



INTRODUCTION

Superhydrophobicity/superoleophobicity and associated self-cleaning and contamination-resistant surface properties have shown enormous potential in widely diverse application fields ranging from antisticking and drag reduction to corrosion resistance, energy conversion and protection of electronics.^{1–5} Fabrics imbued with this super liquid repellency are particularly useful for the development of protective clothing which offers the wearer excellent protection against toxic, corrosive, or flammable liquids, while still maintaining breathability and comfort, besides the applications in the aforementioned areas.

Despite the significant progress made in developing superhydrophobic and superoleophobic surfaces, some challenges still remain that hinder their effective, widespread use in practice. One of the challenges faced by the existing superoleophobic surfaces is the poor repellency to low surface tension fluids, especially those with a surface tension less than 25 mN/m (also referred to as ultralow surface tension in this paper), such as ethanol. However, ultralow surface-tension fluids are used widely in our daily life and industry (a list of examples is provided in the Supporting Information).

Another important challenge is the durability. Most of the existing superhydrophobic surfaces have low durability.⁶ Strategies that have been developed to improve the durability includes cross-linking the coating layer,^{7–9} creating multiscaled roughness on the substrate,¹⁰ establishing chemical bonds between the coating and substrate,¹¹ introducing a bioinspired self-healing function,^{12,13} or endowing the coating with an elastomeric nanocomposite structure.¹⁴ Self-healing is of particular interest to improving durability because any coating,

no matter how durable, is susceptible to physical and chemical damages.

Several self-healing superhydrophobic or superamphiphobic (both superhydrophobic and superoleophobic) coatings have been reported, for example, by chemical vapor deposition of fluoroalkyl silane on a layer-by-layer assembled porous surface on hard substrate,¹² infusing a low surface energy liquid into the intrinsic pores of anodized alumina,¹³ mimicking the formation of a “superslippery” film using a fibrous mat containing low surface energy fluid,¹⁵ adding fluoroalkyl silane coupling agent to thermoplastic polymeric coating,^{16,17} or by using highly fluorinated crystalline fusible wax incorporated with colloidal particles.¹⁸ However, most of the works on self-healing superhydrophobic/superoleophobic coatings only demonstrated the sole ability to self-heal either chemical or physical damage. Liquid repellent coatings having self-healing ability against both physical and chemical damages provide comprehensive protection in various application environments, but have not demonstrated in the research literature.

In the previous work, we also reported a self-healing superamphiphobic fabric coating that was prepared from hydrolyzed fluoroalkyl silane (FAS) containing well-dispersed fluorinated-decyl polyhedral oligomeric silsesquioxane (FD-POSS).¹⁶ The coating showed remarkable self-healing ability against chemical damages. The coated fabric showed relatively low repellency to low surface tension liquids.

Herein, we report that a fabric after being treated with a hydrophobic nanoparticle and FAS/FD-POSS shows a novel

Received: July 22, 2013

Accepted: September 27, 2013

Published: September 27, 2013

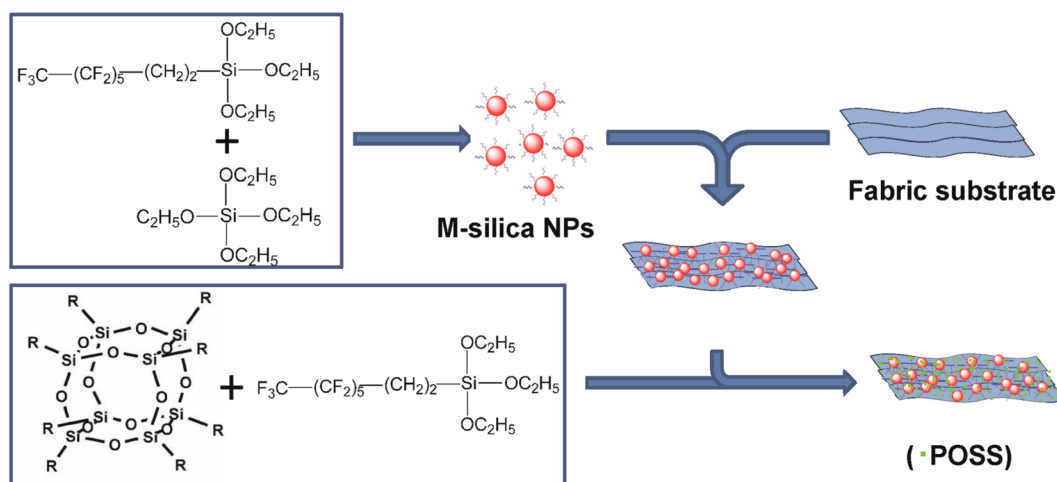


Figure 1. Chemical structures of coating materials and procedure for coating treatment.

multi-self-healing ability against both physical damages (e.g., blade scratching, sandpapering, and abrasion) and chemical damages. The presence of nanoparticles in the coating exceptionally enhanced the liquid repellency of the coating, especially to ultralow surface-tension liquids including ethanol. The significant difference of this work to our previous study is that hydrophobic nanoparticles are added to the coating, which leads to considerable enhancement in both liquid repellency and self-healing to physical damages.

EXPERIMENTAL DETAILS

Materials. Tetraethylorthosilicate (TEOS, 98%), 1H,1H,2H,2H-perfluorodecyltriethoxysilane ($C_{16}H_{19}F_{17}O_3Si$), ethanol (AR), and ammonium hydroxide (28% in water) were obtained from Aldrich. Tridecafluorooctyl triethoxysilane (FAS, Dynasylan F 8261), was supplied by Degussa. All chemicals were used as received. Fluoroalkyl surface-modified silica nanoparticles (FS-NPs) and fluorinated decyl polyhedral oligomeric silsesquioxane (FD-POSS) were synthesized according to our previously reported procedures.^{19,20} Commercial polyester fabric (plain weave, 165 g/m², thickness = 500 μ m) was used.

Coating Procedure. A two-step wet-chemistry coating method was employed to treat the fabrics. In the first step, fabric substrate was immersed into the freshly made FS-NPs/ethanol solution for 5 min. After drying at room temperature to remove ethanol and ammonium hydroxide, the coated fabric was further heated at 110 °C for 1 h. In the second step, FD-POSS (1.0 g) was dissolved in FAS (5.0 g) to form a clear viscous solution, which was then dispersed into 100 mL ethanol. The solution was directly applied to fabric using a dip-coating method. The coated fabric was finally dried at 140 °C for 30 min. Details for making the coating solutions from the first and second step treatment were reported in our previous papers.^{16,19}

Martindale Abrasion. Martindale abrasion test performed according to Standard ASTM D4966, under a commercial Martindale abrasion tester (I. D. M Instrument Design & Maintenance). The fabric sample was mounted on a dynamic disk which was brought into contact with an abradant underneath. The abradant was mounted on a separate motionless disk. Pressure was applied by adding weights onto the upper shaft. During testing, the dynamic disk was rotated on its axis, at the same time as following a circular path across the abradant surface. Untreated fabric was used as the abradant. During the test, 12 kPa of loading pressure was employed, which was often used to evaluate coated fabrics for heavy duty upholstery usages.

Washing Durability. The washing durability was evaluated by reference of the washing procedure described in the AATCC (American Association of Textile Chemists and Colorists) Test Method 61-2006 test No. 2A. The test was performed using a standard

laundering machine (Fong, Fong's National Engineering CO.LTD, Hong Kong, China) equipped with 500 mL (75 mm \times 75 mm) stainless-steel lever-lock canisters. The fabric sample (size, 50 mm \times 150 mm) was laundered in a 150 mL aqueous solution containing 0.15% (w/w) AATCC standard reference detergent WOB and 50 stainless steel balls. During laundering, the temperature was controlled at 49 °C, and the stirring speed was 40 ± 2 rpm. After 45 min of laundering, the laundered sample was rinsed with tap water, and then dried at room temperature without spinning. The contact angle and sliding angle were then measured. This standard washing procedure is equivalent to five cycles of home machine launderings. For convenience, we used the equivalent number of home launderings in this work.

Blade Scratching Test. The blade scratching was performed on a purpose made setup. The coated fabric sample was placed on a flat smooth plate. A flat blade was mounted vertically on a frame with the blade edge in close contact to the top surface of the fabric sample. A 0.8 kg weight was loaded on the blade, which was not sufficient pressure to cut the fabric. The blade was then dragged in a direction perpendicular to the length of the blade with 100 drags of the blade being a "cycle".

Self-Healing of Physical Damages. Self-healing was performed by heating the damaged fabric samples at 140 °C for 30 min.

Vacuum Plasma Treatment (Chemical Damage). The coated fabrics were subjected to a vacuum plasma treatment using a purpose made plasma machine consisting of a vacuum chamber, a radio frequency plasma generator (T&C Power Conversion, Inc. AG0201HV), an electrode system, and a gas supplying system. For each plasma treatment, 5 min of plasma treatment under a power of 19 W was employed. Such a plasma treatment can make fabrics completely hydrophilic and oleophilic (contact angle, 0°).

Self-Healing of Chemical Damages. The plasma treated fabric was heated at 140 °C for 5 min.

Air Permeability. Air permeability was examined by using an FX 3300 air permeability tester according to the Standard (SIST EN ISO 9237-1999). All air permeability values reported represent the mean of five measurements.

Water Vapor Permeability. Water vapor permeability (WVP) was tested using the International Standard Test methods for water vapor transmission of materials (E96/E96M-10).

Other Characterizations. Scanning electron microscopy (SEM) images were taken using an SEM Supra 55VP instrument operated at an acceleration voltage of 5.0 kV. Atomic force microscopy (AFM; Cypher, Asylum Research) was used to measure surface roughness. Transmission electron microscopy (TEM; JEM-200 CX JEOL, Seike Instrument) was used to observe the coated films. Contact angle (CA) measurements were carried out on a contact angle goniometer (KSV CAM 101) using liquid droplets of 5 μ L in volume. Fourier transform

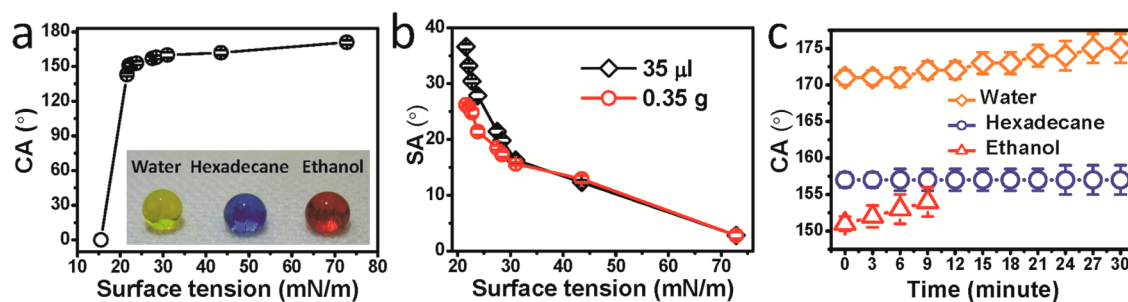


Figure 2. (a,b) Dependency of (a) CA (the photo inset shows yellow-colored water, blue-colored hexadecane, and red-colored ethanol droplets on the coated fabrics; the addition of the dyes to the liquids had little influence on the repellency) and (b) SA of the coated fabric on the surface tension of liquids. (c) CA of water, hexadecane, and ethanol with time.

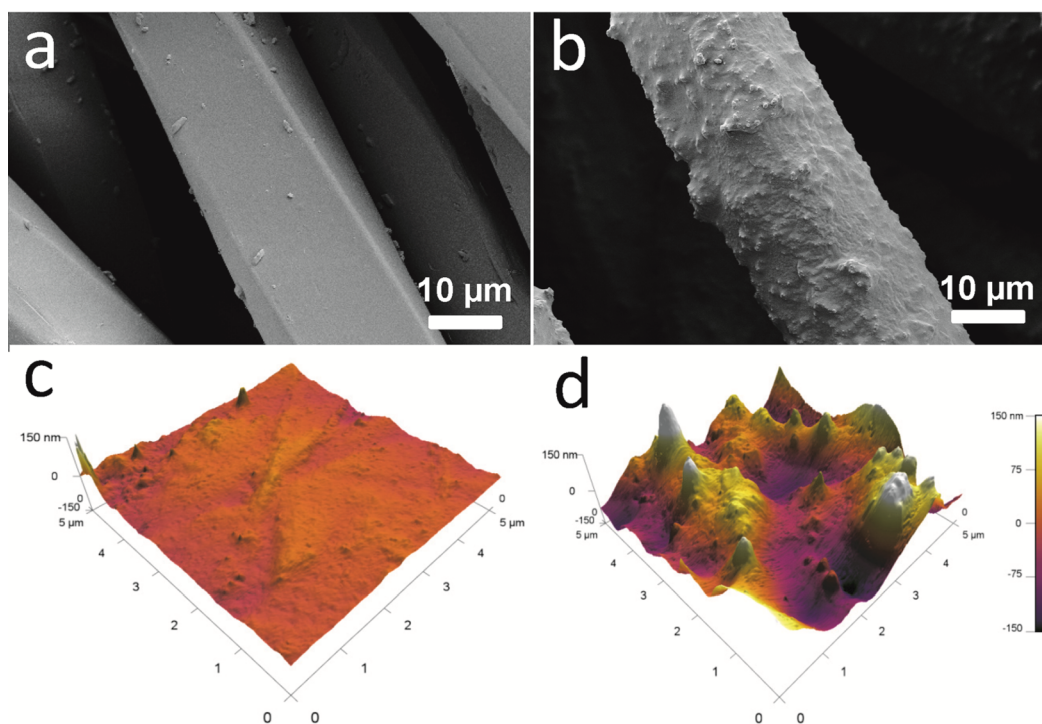


Figure 3. (a,b) SEM images of (a) uncoated and (b) coated polyester fibers. (c,d) AFM images of (c) uncoated and (d) coated polyester fibers.

infrared (FTIR) spectra were recorded on a Bruker VERTEX 70 instrument in ATR mode at a resolution of 4 cm^{-1} accumulating 32 scans. Optical profilometry images were taken using a Bruker Contour GT-K1 3D optical microscope. Scratches were made in the FS-NFs/FD-POSS/FAS coating by use of a scalpel blade by hand with a minimum of pressure applied. The sample was heated using a peltier element.

RESULTS AND DISCUSSION

Figure 1 shows the chemical structures of the materials used for making the coating solutions and the fabric treatment procedure. A fluoroalkyl surface-modified silica nanoparticle (FS-NP), a fluorinated decyl polyhedral oligomeric silsesquioxane (FD-POSS) and a fluoroalkyl silane (FAS), which both were developed in our previous work,^{16,19} were used as the coating materials. They were applied onto the fabric substrate using a two-step dip-coating method.

After coating treatment, the fabric showed a considerable increase in its liquid repellency. As illustrated in Figure 2a, water, hexadecane and anhydrate ethanol droplets ($10\ \mu\text{L}$) form round balls on the treated fabric surface with a CA of

171° , 157° , and 151° , respectively. Further investigation with liquids over a wide range of surface tensions indicated that the liquid CA remained above 150° when the liquid had a surface tension greater than 22.1 mN/m . The CA for liquids with a surface tension below 22.1 mN/m reduced rapidly with decreasing surface tension. These results clearly indicate that the FS-NP/FD-POSS/FAS coated fabric is superamphiphobic and its super repellency covers some ultralow surface-tension liquids, such as ethanol and acetone.

The contact angle hysteresis of the coated fabric was also studied and expressed as sliding angle (SA). The dependency of SA on the surface tension of liquids was tested and shown in Figure 2b. To avoid the influence from droplet weight and size, SAs under constant droplet size ($35\ \mu\text{L}$) and constant droplet weight (0.35 g) were both measured. The SA increased with decreasing fluid surface tension. The SA value based on constant weight was smaller than that based on the constant volume for fluids of less than 30 mN/m surface tension, while above 30 mN/m there was no significant difference. This difference in the SA result between weight and volume can be

attributed to the different density of the liquids (see the Supporting Information).

The excellent liquid repellency of the coated fabric was further proven by leaving water, hexadecane, and ethanol drops (10 μ L) on its surface for extended periods of time, and recording the CA change. As shown in Figure 2c, the CA increases with time for all liquid droplets at room temperature. The CA for water and hexadecane increased respectively to 171° and 157° over 30 min staying on the coated fabric at room temperature. The ethanol droplet evaporated off completely in 10 min because of its high volatility. Despite that, the ethanol droplet increased its contact angle constantly with time before completely evaporating.

The super-repellency was also examined by immersing the coated fabric in a liquid for certain period of time (see the Supporting Information). As expected, the fabric in water remained dry for many days, while it became wetted in a shorter time when immersion in an oil fluid. In ethanol, the fabric was wetted after 1.5 h of immersion. However, its surface repellency was restored once dry at room temperature.

Figure 3a and b provides the morphological information of the polyester fabric before and after the coating treatment. Without coating, the polyester fibers showed a smooth surface (Figure 3a) (more SEM images can be found in the Supporting Information). The coated fibers are much rougher, with particulate protrusions scattered on the surface (Figure 3b). AFM imaging verified that the fiber significantly increased its surface roughness after coating (Figure 3c and d). The root-mean-square (RMS) roughness measured based on the AFM images was 116 nm for the coated fiber in contrast to the uncoated fiber with an RMS roughness of just 2 nm. The TEM image shown in the inset of Figure 3b reveals that FS-NP coating layer is covered with a thin layer of FD-POSS/FAS coating. The overall coating layer was approximately 200 nm in thickness.

The chemical components of the coating layer were verified by FTIR (Supporting Information). After coating treatment, the vibration peaks at 1200 and 1150 cm^{-1} appeared, which were assigned to the C–F stretching vibrations of the fluorinated alkyl chains. The peaks appearing at 1087 and 810 cm^{-1} correspond to the Si–O–Si asymmetric and symmetric vibrations, respectively. The absorption peaks around 949 and 1100 cm^{-1} were attributable to Si–OH bending and C–O stretching vibrations, respectively. The FTIR results confirmed that the fabric was covered with a layer of silica coating enriched with fluoroalkyl groups after the coating treatment.

From our previous studies and throughout the literature,^{14,21} it is well-known that a low surface energy in addition to a hierarchical, micro/nanoroughness is required for super-amphiphobicity. The low surface energy is provided here by the fluoroalkyl chains, as confirmed by FTIR, the microscale roughness is inherent in the fabric weave and the addition of nanoparticles provided the nanoscale roughness.

Washing is an important cause of degradation to superhydrophobic coatings during their practical uses. Fabric during washing undergoes mechanical stresses in addition to chemical agents. The synergistic effect of chemical and physical actions accelerates the detachment of coating layer on fiber substrate. Under a standard machine laundry process, the coated fabric did not change the CA to water, hexadecane or ethanol after 200 cycles of washing (Figure 4a). However, the SA was increased to 4.5°, 36.7°, and 47.5° for water, hexadecane, and

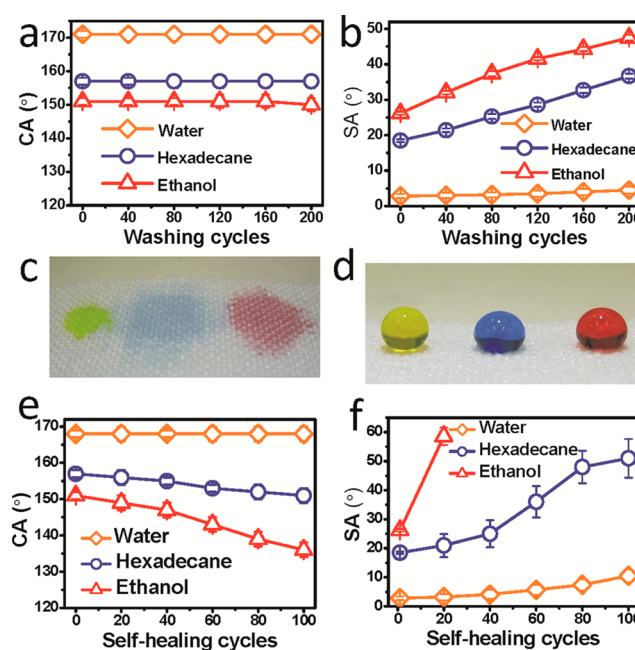


Figure 4. (a) CA and (b) SA versus washing cycles, (b,c) photos of water, hexadecane, and ethanol drops on the coated fabric (b) after plasma treatment and (c) the plasma treated fabric after heating at 140 °C for 5 min. (d) Effect of plasma and self-healing cycles on CA and SA of the FS-NP/FD-POSS/FAS coated fabric (here one “plasma and self-healing cycle” is defined as 5 min plasma treatment followed by 5 min heating at 140 °C).

ethanol, respectively (Figure 4b). The result suggests that the coating is durable enough to withdraw gentle physical-chemical actions.

To prove the self-healing of chemical damages, the FS-NP/FD-POSS/FAS coated fabric was damaged deliberately by a plasma treatment in vacuum using air as the gas source. Such a treatment can introduce polarity groups (e.g., hydroxyl or carboxylic groups) to the fabric surface. As a result, the treated fabric became amphiphilic with contact angle of 0° to both water and oil fluids. However, when the plasma-treated fabric was heated at 140 °C for just 5 min, its liquid repellency was restored (Figure 4c and d). The self-healing was repeatable and can perform many times. Figure 4e and f show the effect of plasma and self-healing treatment cycles on the CA and SA. After 100 cycles of plasma and self-healing, the fabric still maintained the superphobicity to water and hexadecane. Although the fabric lost the super repellency to ethanol after the first five cycles, the fabric was still repellent to ethanol after 100 cycles of the plasma and self-healing treatment. In comparison to FD-POSS/FAS coating,¹⁶ the FS-NP/FD-POSS/FAS coating is much more robust in the self-healing ability to recover superoleophobicity from chemical damage. This is presumably because of the nanocomposite structure of the coating layer. The silica nanoparticles function to reduce plasma etching because of the excellent stability, hence protecting FD-POSS/FAS. Self-healing yield (η) can be estimated by the equation, $\eta = \theta_{\text{after}}/\theta_{\text{before}}$ (where θ_{before} and θ_{after} are contact angles before the damage and after self-healing, respectively). For each plasma treatment cycle, the self-healing yield was very high, greater than 98% for water and oil fluids studied. The overall η for the entire 100 cycles of plasma and self-healing treatment was 100% and 90%, respectively, for water and ethanol.

Apart from chemical damage, physical damages such as scratching with a sharp blade, abrasion with sandpaper, and Matindale abrasion were employed to test durability and self-healing ability of the coated fabric. When the coated fabric was scratched with a sharp blade, its liquid repellency decreased. Figure 5a–c shows the coated fabric during blade scratching

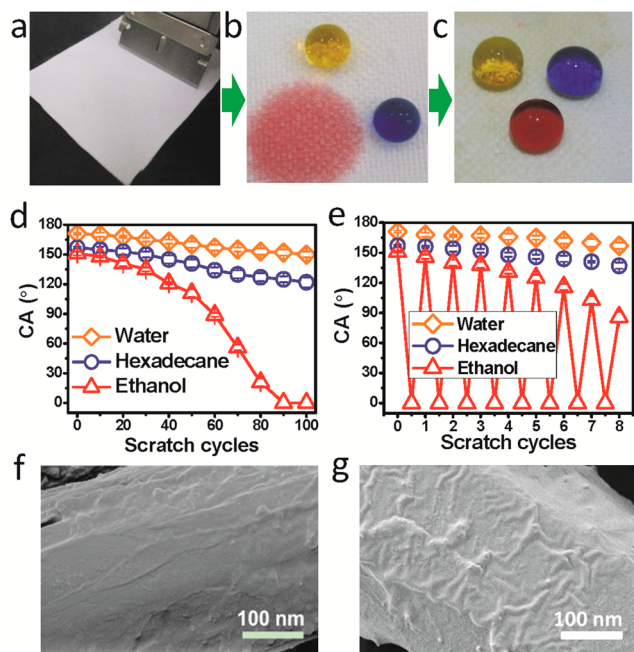


Figure 5. (a–c) Photos to show (a) the method of scratching fabric with a sharp blade, (b,c) colored water, hexadecane, and ethanol drops on the coated fabric (b) after the first blade scratching cycle (100 scratches) and (c) after blade scratching and heat treatment at 140 °C. (d) CA change with the first 100 blade scratches. (e) CA change with blade-scratching and heating cycles. (f,g) SEM images of the coated fabric (f) after blade scratching (100 scratches) and (g) heat treatment.

and liquid droplets on the scratched fabric. The effect that the number of scratches performed on the CA is shown in Figure 5d. With increasing number of scratches, the fabrics CA gradually reduced. After 100 scratches were performed, the ethanol CA reduced to 0°, while the CA for water and hexadecane reduced to 150° and 120°, respectively.

It was very interesting to note that the scratch-induced degradation in liquid repellency was repairable. After heat treatment of the scratched fabric at 140 °C for 30 min, the CA changed to 168°, 156°, and 146° for water, hexadecane, and ethanol, respectively. This thermally activated self-healing process was repeatable. As shown in Figure 5e, after eight scratching and healing cycles (in each cycle the fabric was scratched 100 times), the ethanol CA reduces to 83°. For the first eight scratch and self-healing cycles, the self-healing yield of individual cycle changed from 96.7% to 83.5% for ethanol (overall η around 60%). The η for water and hexadecane had higher values.

Under SEM, the coated fibers looked smoother after blade-scratching and in some areas the nanoparticulate protrusion of the surface structure was completely removed (Figure 5f and g). Some fibers broke after scratching, although the blade did not cut the fibers directly. The blade scratching removed a part of coating material and even some sections of fibers from the

fabric. This led to the exposure of the fiber substrate in some scratched areas, hence reducing the liquid repellency.

Similarly, the coated fabric also self-healed after being abraded with a piece of fine sandpaper (sandpaper 1200 grit 9" × 11"). The coated fabric reduced its liquid repellency after sandpaper abrasion, particularly to ethanol which had its CA reduced to 0°. When the sandpapered fabric was heated at 140 °C for 30 min, its liquid repellency was recovered despite some reduction in the CA value (see the Supporting Information). The healing from this physical damage is also repeatable, despite being hindered by trace amounts of abradant detaching from the sandpaper, contaminating the abraded surface. For comparison, FAS/FD-POSS coated fabric was also subjected to a similar test, but the self-healing ability was very low presumably due to the thin, soft coating layer. The nanoparticles in the FS-NP/FD-POSS/FAS coating function to reinforce the coating to withstand the severe scratches.

The above results demonstrate the ability of the coated fabric to self-heal its super liquid repellency after severe physical damages. For fabrics in everyday routine uses, the physical damages occur more likely from gentle abrasion, such as when coming into contact with other fabric. The abrasion durability of the coated fabric was tested using the Martindale method, a standard method to test the abrasion resistance of fabrics. In our case, the abrasion test was performed under a loading of 12 kPa using uncoated polyester as the abradant, which is often used to simulate real-world heavy duty wear.

The change in liquid repellency with abrasion cycles is presented in Figure 6a and b. After 20 000 cycles of abrasion,

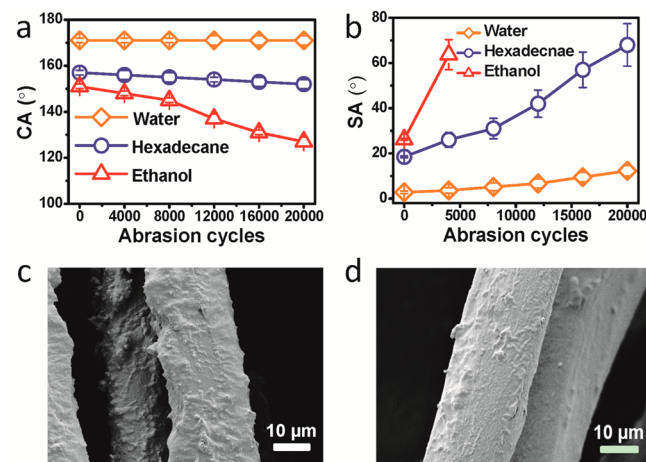


Figure 6. (a) CA and (b) SA change with Martindale abrasion cycles. (c,d) SEM images of the coated fibers after (c) 5000 cycles and (d) 20 000 cycles of Martindale abrasion.

the water CA almost had no change. Alternatively, the CA for hexadecane and ethanol reduced with increasing the abrasion cycles, although the hexadecane CA value was still above 150° after 20 000 cycles of abrasion, the CA for ethanol reduced to 127° after the abrasion (Figure 6a). The SA suffered a larger impact from abrasion testing than the CA. After 20 000 cycles of abrasion, the SA to water and hexadecane increased, respectively, from 2.8° and 18.5° to 12.3° and 68.0° (Figure 6b). A larger increase in SA was observed for ethanol, which reached the test limit of 75° after 5000 cycles of abrasion.

The reduced liquid repellency after abrasion was mainly attributed to reduction in surface roughness. As shown in

Figure 6c and d, after 5000 cycles of abrasion, some nanoparticles were removed from the coating layer, and after 20 000 cycles of abrasion nearly no nanoparticles could be observed from the top surface. Again, the damaged wettability after the Martindale abrasion test was also healable. After 20 000 cycles of abrasion when the coated fabric was heated at 140 °C for 30 min, the CA to water and hexadecane recovered 171° and 152°, respectively. However, the heat treatment could only increase the CA to ethanol to 127°.

The mechanism of self-healing to physical damages was attributed to the movement of coating on the coated surface. To prove this, FS-NP/FD-POSS/FAS was coated on a silicon wafer and the coating film was scratched. The morphology change of the scratched area upon heating and then cooling was recorded (details see Supporting Information). When the surface was heated to 55 °C, the coating became more mobile and the scratch begins to reduce in depth. At 75 °C, the coating became significantly more mobile, and the scratch began to disappear. At 110 °C, the coating melted completely which ensured complete even coverage of the coating. Further cooling of the coating to 90 °C resulted in solidification of the coating layer with the scratch being completely healed.

Here it should be pointed out that the procedure to self-heal physical damages is similar to that for chemical ones, except that self-healing of physical damages takes longer time than that for chemical damages. Both damages can be repaired just in one go of heat treatment at 140 °C for 30 min. It was also noted that C–O stretching vibration appeared in the FTIR spectrum of the coated fabric after both chemical and physical damages (Supporting Information). However, this was originated from different sources. Physical damages lead to the exposure of some substrate (polyester) surface, which contains C–O bonds. For the chemical damages, C–O bonds are introduced due to the plasma treatment.

Apart from the excellent liquid repellency and multi-self-healing ability, the coating was found to have a very small influence on the permeability and color of the fabric (see the Supporting Information). The coating treatment led to a slight decrease in the air permeability from 36.44 to 33.82 cm³/cm²/s, and the water vapor permeability dropped from 7500 to 7050 g/m²/day.

CONCLUSION

A two-step coating technique has been developed to endow fabrics with remarkable superamphiphobicity and multi-self-healing ability. The treated fabrics show exceptional liquid repellency to low surface tension liquids including ethanol. The coating is also durable to withstand 200 cycles of wash and 5000 cycles of Martindale abrasion without apparently changing the superamphiphobicity. The coating has self-healing ability against both chemical and physical damages. This highly robust, superamphiphobic fabric may find applications for the development of “smart” functional textiles for various applications in personal protection, self-cleaning, defense, healthcare, and daily life.

ASSOCIATED CONTENT

Supporting Information

Details on commonly used ultralow surface tension fluids and their applications, self-healing of sandpaper abrasion, SEM images, FTIR spectra, photos to show wettability and fabric appearance. This material is available free of charge via the Internet at <http://pubs.acs.org>.

AUTHOR INFORMATION

Corresponding Author

*E-mail: tong.lin@deakin.edu.au.

Notes

The authors declare no competing financial interest.

ACKNOWLEDGMENTS

Funding support from Australia Research Council through a Discovery project and Deakin University under its Central Research Grant scheme is acknowledged.

REFERENCES

- (1) Deng, X.; Mammen, L.; Butt, H. J.; Vollmer, D. *Science* **2011**, *335*, 67–70.
- (2) Tuteja, A.; Choi, W.; Ma, M.; Mabry, J. M.; Mazzella, S. A.; Rutledge, G. C.; McKinley, G. H.; Cohen, R. E. *Science* **2007**, *318*, 1618–1622.
- (3) Li, X. M.; Reinhoudt, D.; Crego-Calama, M. *Chem. Soc. Rev.* **2007**, *36*, 1350–1368.
- (4) Zhang, F.; Zhao, L.; Chen, H.; Xu, S.; Evans, D. G.; Duan, X. *Angew. Chem., Int. Ed.* **2008**, *47*, 2466–2469.
- (5) Yao, X.; Song, Y.; Jiang, L. *Adv. Mater.* **2011**, *23*, 719–734.
- (6) Quéré, D. *Annu. Rev. Mater. Res.* **2008**, *38*, 71–99.
- (7) Deng, X.; Mammen, L.; Zhao, Y.; Lellig, P.; Müllen, K.; Li, C.; Butt, H.-J.; Vollmer, D. *Adv. Mater.* **2011**, *23*, 2962–2965.
- (8) Verho, T.; Bower, C.; Andrew, P.; Franssila, S.; Ikkala, O.; Ras, R. H. A. *Adv. Mater.* **2011**, *23*, 673–678.
- (9) Han, J. T.; Zheng, Y.; Cho, J. H.; Xu, X.; Cho, K. *J. Phys. Chem. B* **2005**, *109*, 20773–20778.
- (10) Zimmermann, J.; Reifler, F. A.; Fortunato, G.; Gerhardt, L. C.; Seeger, S. *Adv. Funct. Mater.* **2008**, *18*, 3662–3669.
- (11) Deng, B.; Cai, R.; Yu, Y.; Jiang, H.; Wang, C.; Li, J.; Li, L.; Yu, M.; Li, J.; Xie, L.; Huang, Q.; Fan, C. *Adv. Mater.* **2010**, *22*, 5473–5477.
- (12) Li, Y.; Li, L.; Sun, J. *Angew. Chem., Int. Ed.* **2010**, *49*, 6129–6133.
- (13) Wang, X.; Liu, X.; Zhou, F.; Liu, W. *Chem. Commun.* **2011**, *47*, 2324–2326.
- (14) Zhou, H.; Wang, H.; Niu, H.; Gestos, A.; Wang, X.; Lin, T. *Adv. Mater.* **2012**, *24*, 2409–2412.
- (15) Wong, T. S.; Kang, S. H.; Tang, S. K. Y.; Smythe, E. J.; Hatton, B. D.; Grinthal, A.; Aizenberg, J. *Nature* **2011**, *477*, 443.
- (16) Wang, H.; Xue, Y.; Ding, J.; Feng, L.; Wang, X.; Lin, T. *Angew. Chem., Int. Ed.* **2011**, *50*, 11433–11436.
- (17) Zhou, H.; Wang, H.; Niu, H.; Gestos, A.; Wang, X.; Lin, T. *Adv. Mater.* **2012**, *24*, 2409–2412.
- (18) Pureskiy, N.; Stoychev, G.; Synytska, A.; Ionov, L. *Langmuir* **2012**, *28*, 3679–3682.
- (19) Wang, H.; Fang, J.; Cheng, T.; Ding, J.; Qu, L.; Dai, L.; Wang, X.; Lin, T. *Chem. Commun.* **2008**, *44*, 877–879.
- (20) Xue, Y.; Wang, H.; Zhao, Y.; Dai, L.; Feng, L.; Wang, X.; Lin, T. *Adv. Mater.* **2010**, *22*, 4814.
- (21) Bhushan, B.; Jung, Y. C.; Koch, K. *Philos. Trans. R. Soc., A* **2009**, *367*, 1631–72.